THE JOURNAL OF PHYSICAL CHEMISTRY B

Article

pubs.acs.org/JPCB

Two-Photon and Time-Resolved Fluorescence Spectroscopy as Probes for Structural Determination in Amyloid-β Peptides and Aggregates

Travis B. Clark,[†] Marcin Ziółkowski,[‡] George C. Schatz,[‡] and Theodore Goodson, III*,[†]

[†]Department of Chemistry, The University of Michigan, 930 North University Avenue, Ann Arbor, Michigan 48109, United States

[‡]Department of Chemistry, Northwestern University, 2145 Sheridan Road, Evanston, Illinois 60208-3113, United States

Supporting Information

ABSTRACT: The development of new sensitive methods for the detailed collection of conformational and morphological information about amyloids is crucial for the elucidation of critical questions regarding aggregation processes in neurodegenerative diseases. The combined approach of two-photon and time-resolved fluorescence spectroscopy described in this report interrogates the early conformational dynamics seen in soluble oligomers of amyloid-β(1−42). Concentration-dependent aggregation studies using two-photon absorption show enhanced sensitivity toward conformational changes taking place in the secondary structure of the amyloid peptide as aggregation proceeds. Fluorescence lifetimes and changes in anisotropy values indicate Förster-type energy transfer occurring as a function of aggregation state. The sensitivity of our two-photon methodology is compared to that of circular dichroism (CD) spectroscopy, and the results indicate that the two-photon absorption cross-section method exhibits superior sensitivity. A theoretical model is developed that, together with electronic structure calculations, explains the change in cross section as a function of aggregation in terms of interacting transition dipoles for aggregates showing stacked or parallel structures. This suggests that the two-photon method provides a sensitive alternative to CD spectroscopy while avoiding many of the inherent challenges particular to CD data collection. The implication of this finding is significant, as it indicates that a two-photon-based technique used in conjunction with time-resolved fluorescence might be able to reveal answers to conformational questions about amyloid-β(1−42) that are presently inaccessible with other techniques.

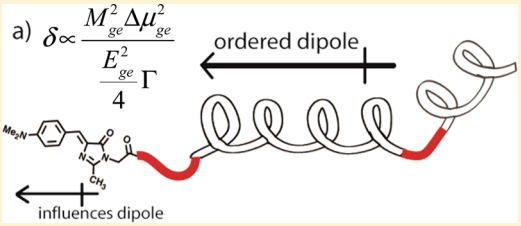

INTRODUCTION

Conformational changes associated with the aggregation of proteins are vital to understanding the fundamental events involved in the development of neurodegenerative diseases,[1,2] such as Alzheimer's disease (AD). A number of techniques have been utilized (Figure 1) to study the various stages of amyloid aggregation from small monomers[3] to large fibrils, including circular dichroism (CD),[4] fluorescence of amyloid-binding dyes,[5] mass spectrometry (MS),[6] and physical imaging methods.[7,8] Solution-based techniques (CD, MS) are best implemented in the earlier stages of aggregation in which soluble oligomer structures and protofibrils[9] predominate. Other techniques, such as atomic force microscopy (AFM) and fluorescence monitoring of ThT-type fibril binding dyes are somewhat better suited for the larger aggregate structures found toward the later stages of amyloid fibrillization. Fluorescence-based methodologies utilizing either extrinsic[10] or intrinsic[11] fluorescence labels have been explored as alternative techniques with the capability of specifically studying oligomeric interactions of the early intermediates.

A combined approach, using nonlinear optical spectroscopy and time-resolved fluorescence studies to examine the inter- and intramolecular interactions as a function of conformation, provides a powerful avenue for probing aggregation in peptide systems. Of particular importance is the potential to have higher two-photon absorption (TPA) cross sections due to cooperative enhancement from interchromophore interactions.[12,13] The high spatial selectivity afforded by two-photon excitations has further led to an exploration of TPA as a tool for understanding the complex interactions taking place in biological systems.[14−16] TPA techniques are promising for the continued study of conformational changes and aggregation of peptides; however, the development of better environmentally sensitive TPA chromophores is an important limitation on the generation of fundamental data that can be used to answer critical questions about amyloid peptides.

In this report, the dynamics of early aggregation processes in amyloids is investigated. We have prepared a new analogue of the green fluorescence protein chromophore designed to have strong environmental sensitivity and a large TPA cross section that can be utilized in ultrafast spectroscopic investigations. To study aggregation, the two-photon chromophore was labeled at the N-terminus of the amyloid-β(1−42) [Aβ(1−42)] peptide. A dimethylamino-substituted GFP-type chromophore (denoted

Received: January 24, 2014
Revised: February 6, 2014
Published: February 6, 2014

   dx.doi.org/10.1021/jp500883s | J. Phys. Chem. B 2014, 118, 2351−2359

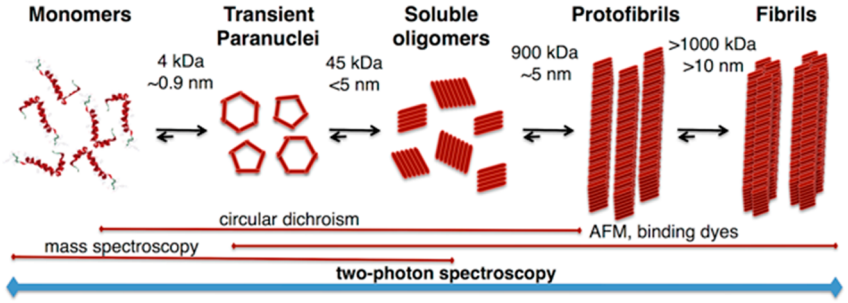

Figure 1. Schematic representation of the broad classification of amyloid fibrillization and some techniques commonly associated with its characterization.

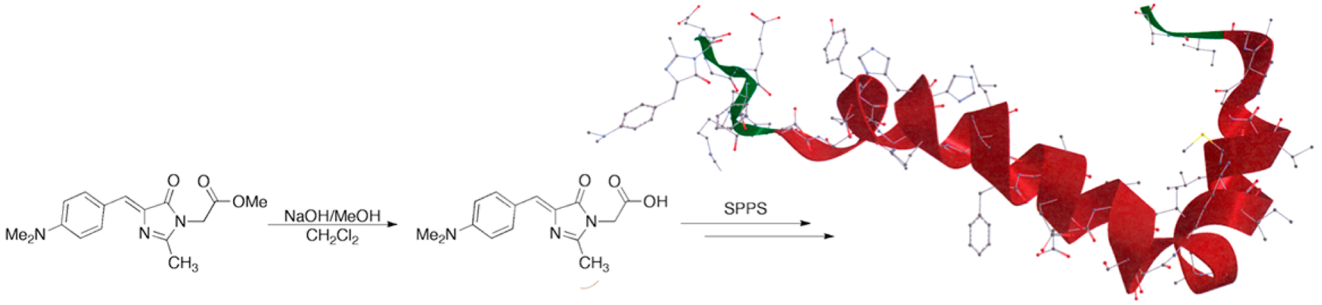

Figure 2. Synthetic scheme for the generation of DMC-labeled amyloid-β(1−42). A model representation of the DMC N-terminus-labeled amyloid-β(1−42) is shown.

DMC) was synthesized by a previously published route[17] and covalently attached to the peptide following solid-phase peptide synthesis (Figure 2). In this way, we are able to introduce the fluorophore into a region of the peptide that is not centrally involved in the aggregation, ensuring that it does not interfere in the process, yet has the flexibility to interrogate nearby changes in the secondary structure of the aggregation-prone region of the peptide. The methodology described herein most appropriately interrogates the early conformational dynamics seen in the regime of monomers and soluble oligomers that is most commonly studied using CD or MS. TPA methods thus provide environmental and conformational information about peptide aggregation that is crucial for understanding the various topographies and morphologies that can be adopted by the early oligomers of Aβ and that can be targeted for therapeutic intervention.

EXPERIMENTAL SECTION

Synthesis. (*Z*)-2-(4-(4-(dimethylamino)benzylidene)-2-methyl-5-oxo-4,5-dihydro-1*H*-imidazol-1-yl)acetic acid (DMC−OH) was synthesized using a method reported in the literature.[18] In a small round-bottom flask, DMC−OMe (260 mg, 0.836 mol) recrystallized from methanol was dissolved in 5 mL of 9:1 CH_2/MeOH, creating a reddish solution. NaOH (1 mL, 2 M in MeOH) was added by syringe. After a period of several minutes, the carboxylate salt precipitated as a solid. The solution was suction-filtered to collect an orange, fluffy solid. The precipitate was washed with additional portions of dichloromethane to remove any residual starting material. Thin-layer chromatography (eluent EtOAc) was used to track the full conversion of the starting material. ^{1}H NMR [400 MHz, dimethyl sulfoxide (DMSO), δ]: 8.066 (Ar—**H**, 2H, d), 6.902 (C—C**H**=C, 1H, s), 6.752 (Ar—**H**, 2H, d), 4.358 (—C**H**$_2$, 2H, s), 3.008 [—N(C**H**$_3$)$_2$, 6H, s], 2.259 (—C**H**$_3$, 3H, s). ^{13}C NMR (100 MHz, DMSO, δ): 15.079 (—C**H**$_3$), ∼39 obscured under DMSO peak [—N(C**H**$_3$)$_2$], 41.228 (—C**H**$_2$), 111.687 (H**C**=C—), 121.420 (Ar), 127.231 (Ar, 2C), 133.977 (Ar, 2C), 151.447 (Me$_2$N—**C**), 159.448 (N=**C**), 169.328 (O=**C**), 169.778 (—**C**OOH).

Amyloid-β(1−42) was subsequently synthesized by solid-phase peptide synthesis (Anaspec, Inc.), and DMC−OH was covalently attached at the N-terminus of the peptide (Figure 2). High-resolution MS (m/z): calcd for DMC-Aβ(1−42), 4931.6; found, 4931.7 (Figure S1, Supporting Information).

Aβ Sample Preparation. To disaggregate the Aβ and generate monomeric α-helical structures, a stock solution of the DMC-Aβ(1−42) was prepared by dissolving 1 mg of the peptide into 1.4 mL of hexafluoroisopropanol (HFIP) and subsequently stored in a freezer at −20 °C before use. The concentration of this stock solution (1.44×10^{-4} M) was verified over time using the determined molar extinction coefficient (ε_{475} = 10985 M^{-1} cm^{-1}). For concentration-dependent aggregation measurements, peptide samples of various concentrations were prepared by dilution from the stock solution and maintained in a cosolvent of 20:80 HFIP/phosphate buffer solution (PBS). These solutions were then stored in sealed vials in a desiccator. Aggregation solutions were prepared using phosphate buffer solution (PBS, without Ca^{2+} and Mg^{2+}). Solutions were observed beginning immediately after preparation.

Steady-State Measurements. Absorption and emission spectra were recorded on an Agilent 8341 spectrophotometer and a Fluoromax-2 fluorimeter, respectively. Quartz cells of 0.4-cm path length were utilized for all measurements unless otherwise noted. Fluorescence quantum yields were obtained using fluorescein as the known fluorescence standard and at optical densities below 0.1 near the maximum absorption. All CD spectra were recorded with an Aviv model 202 circular dichroism spectrometer at 25 °C using a bandwidth of 1.0 nm and a wavelength step of 0.5 nm.

dx.doi.org/10.1021/jp500883s | J. Phys. Chem. B 2014, 118, 2351−2359

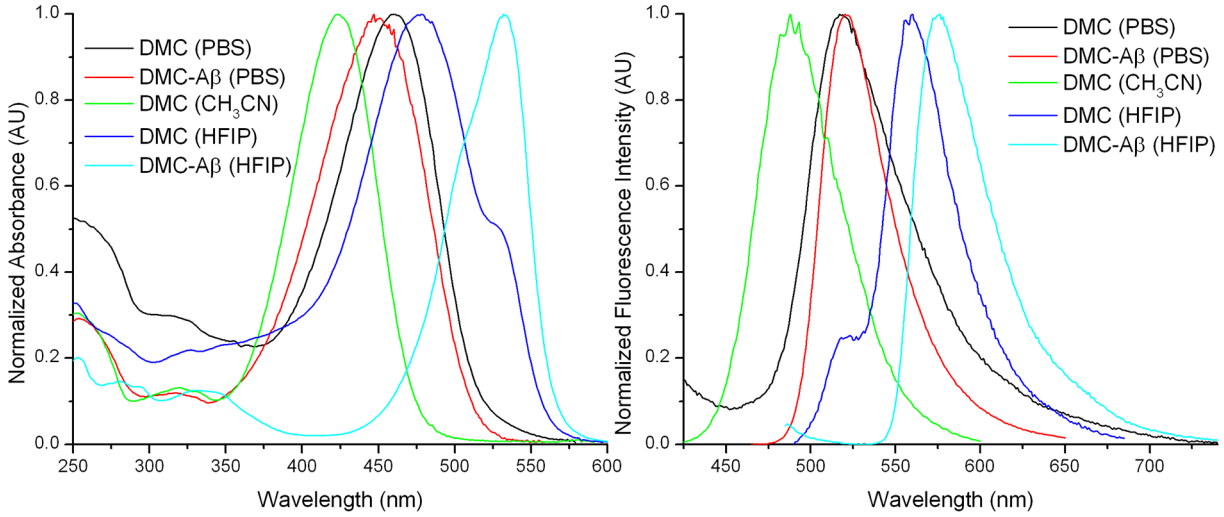

Figure 3. Steady-state absorption and emission curves for DMC-Aβ(1−42) and DMC in different solvent conditions. The curves are as follows: (black) DMC, PBS; (red) DMC-Aβ, PBS; (green) DMC, acetonitrile; (blue) DMC, HFIP; and (cyan) DMC-Aβ, HFIP. All peptide solution spectra were recorded immediately following preparation. Emission data were collected through excitation at the respective absorption maxima.

Table 1. Comparison of Photophysical Characteristics of DMC and DMC-Aβ(1−42) in PBS

	absorbance[a] λ_{max} (nm)	emission[a] λ_{max} (nm)	molar extinction coefficient ε (M^{-1} cm^{-1})	concentration c (M)	QY Φ	TP "action" cross section $\Phi\delta$ (GM)	TPA cross section δ (GM)
DMC-Aβ(1−42)	460	520	10900[a]	0.5×10^{-6}	3.0×10^{-4}	0.150	540
DMC	450	520	26000[b]	0.5×10^{-6}	9.5×10^{-4}	0.031	32

[a]Phosphate-buffer solution. [b]Determined for DMC-Aβ(1−42) in HFIP.

Two-Photon Absorption. Two-photon absorption cross sections were measured using the two-photon excited fluorescence (TPEF) method as described elsewhere.[19] A solution of Coumarin 307 in methanol (<10^{-4} M) was used as the TPA reference for studies at 800-nm excitation. A Kapteyn Murnane Laboratories diode-pumped mode-locked Ti:sapphire laser was utilized for sample excitation. The beam was directed onto the sample cell (quartz cuvette, 0.4-cm path length), and the resultant fluorescence was collected perpendicular to the incident beam. A 1-in.-focal-length plano-convex lens was used to direct the collected fluorescence into a monochromator whose output was coupled to a photomultiplier tube. The photons were converted into counts by a photon-counting unit. A logarithmic plot of collected fluorescence photons versus input intensity was verified to yield a slope of 2, indicating a quadratic power dependence.

Ultrafast Time-Resolved Fluorescence Upconversion. The fluorescence upconversion system used for time-resolved measurements of the chromophores has been described previously.[20] Briefly, a Tsunami mode-locked Ti:sapphire (Spectra Physics) laser operated at 120 fs with pulses of ~815 nm (gate pulse) having a repetition rate of 82 MHz was used to generate light of 410 nm (excitation) from second harmonic generation in a β-barium borate crystal. Using an FOG-100 system (CDP Inc.), the gate pulse was channeled through a delay line while the excitation light was upconverted and used to excite the samples. A monochromator detected the second harmonic generation of the gate pulse and emission from the samples, which were amplified on a photomultiplier tube. Fluorescence anisotropy results were collected by changing the polarization of the excitation beam using a Berek compensator to set parallel and perpendicular excitations. The G factor was determined to be 0.96 using a Coumarin 30 reference standard.

RESULTS AND DISCUSSION

Steady-State Spectroscopy. Prior to a detailed study of the Aβ(1−42) aggregation, baseline steady-state studies were performed to characterize the fundamental photophysical properties of the labeled peptide system as compared to those of the isolated chromophore. Different solvent conditions were investigated to examine the changes in absorption and emission spectra (Figure 3). In PBS, significant red shifts to 450 and 520 nm were observed for the absorption and emission, respectively, as compared to the values for the free dye in acetonitrile. The spectrum for the labeled peptide, DMC-Aβ(1−42), was slightly red-shifted to 460 nm as compared to that of the free dye (Table 1). This effect can be attributed to environmental effects arising from the influence of the microenvironment surrounding the chromophore causing a shift in the ground-state absorption. The emission data exhibited a far less pronounced shift, with both systems having a maximum near 520 nm. A subsequent examination of DMC-Aβ(1−42) in HFIP showed large shifts in both the absorption and emission spectra that were significantly greater than those found in PBS, with maxima at 532 and 575 nm, respectively. This effect is attributed to the lessened capacity of HFIP to form hydrogen bonds as compared to water, thus promoting a greater level of intramolecular interactions that might result in lower-energy transitions observed coming from the ground state. The overall steady-state results indicate a high sensitivity of DMC to environmental conditions, especially considering the high relative polarities of the solvents.

Fluorescence quantum yields were determined in buffer solution for both DMC-Aβ(1−42) and DMC. The quantum

dx.doi.org/10.1021/jp500883s | J. Phys. Chem. B 2014, 118, 2351−2359

yield was previously determined for DMC in acetonitrile (3.4×10^{-4});[17] however, the isolated chromophore was found to be slightly more fluorescent in the buffer solution (9.5×10^{-4}). The labeled peptide showed no indications of enhanced fluorescence resulting from the labeling as might have been expected[21] and was actually found to have a quantum yield lower than that of the isolated chromophore (Table 1).

Circular Dichroism Spectroscopy. Circular dichroism (CD) spectroscopy was performed on aggregating solutions with concentrations of of 0.5, 1, 2.5, 5, 10, and 40 μM immediately after their preparation. When compared with the unlabeled peptide, there was no evidence of any effect on the obtained CD spectra for a similarly N-terminus-labeled Aβ peptide, consistent with previous studies.[16,22] Barrow et al. established how changes in secondary structure as the amyloid-β peptide undergoes a conformational change from α-helix to β-sheet are associated with the spectral changes observed in the CD spectrum in composite solutions containing fluorinated alcohols.[4] Our obtained spectra (Figure 4) showed negative

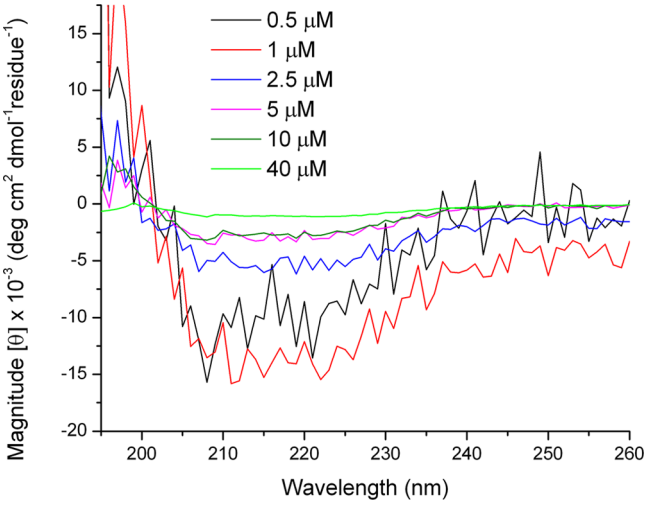

Figure 4. Molar ellipticity data of DMC-Aβ(1−42) aggregating samples immediately after preparation. A solvent blank was subtracted from each, and averages of three spectra were used to construct the plots.

ellipticities with a bimodal peak centered at 208 nm extending to just beyond 220 nm, with the peak shape and intensity dependent on the solvent conditions and peptide concentrations. Higher-concentration solutions had a less pronounced signal, with the magnitude generally increasing as the concentration of the solution was decreased, behavior consistent with a system with higher β-sheet content. As the mean residue ellipticity of the peptide approaches 0, the predominantly α-helical structure of the peptide changes to increasingly larger percentages of β-sheet structure.[4] Values for the mean residue ellipticity at 222 nm were calculated and are listed in Table 2 as a function of concentration. At the lowest studied concentrations (0.5 and 1 μM), a plateauing of the molar ellipticity was noted. Based on the concentrations of these solutions, a decline in sensitivity for samples at 1 μM is not unexpected, given the low optical density of the fluorophore in solution.

Two-Photon Spectroscopy. Two-photon absorption spectroscopy was utilized in studying DMC-Aβ(1−42) as a function of concentration and incubation time. Solutions near

Table 2. Two-Photon Absorption Cross Section and Molar Ellipticity[a] Data Taken over a Range of Concentrations[b]

peptide concentration (μM)	ellipticity (deg cm^2 dmol)	TPA cross section δ (GM)
0.5	9942	540
1	15466	283
2.5	4817	133
5	3027	92
10	2756	108
40	1118	191

[a]Values determined from CD data collected at 222 nm. [b]All data collected immediately after preparation of aggregating solution from stock solution.

biologically relevant concentrations (<1 μM)[3] ranging from 0.5 to 40 μM in PBS were prepared by dilution from a HFIP stock solution to have a final HFIP-to-PBS ratio of 20:80. Initially, we carried out two-photon examinations of the free dye and attached dye−peptide (very low concentrations). This was done to determine the effect of attaching the chromophore to Aβ(1−42). Under excitation at 800 nm, two-photon excited fluorescence of the chromophore was observed and used to determine the overall two-photon absorption cross section. The obtained quadratic dependence of the fluorescence intensity as a function of input power indicated a clear two-photon absorption event (Figure 5). The two-photon absorption cross

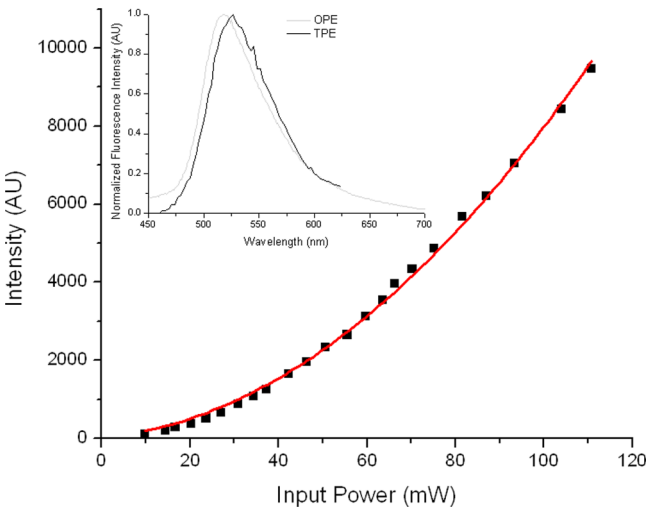

Figure 5. Quadratic dependence of intensity on input power for 40 μM DMC-Aβ(1−42). Inset: Two-photon-excited fluorescence (black) compared to one-photon-excited fluorescence.

section of the Aβ(1−42)−chromophore peptide system was found to be 540 GM for the 0.5 μM solution. Under the same conditions, the isolated DMC was found to have a cross section of 32 GM, almost an order of magnitude smaller than for the peptide system (Table 1). Given the drop in quantum yield, the dye−peptide system shows an impressively large TPA cross section that will be useful for diagnostic applications. The difference between the free dye and the attached dye−peptide system (at very low concentration) can be attributed to changes in the local environment when the dye is introduced into the α-helix of the peptide and, consequently, changes in the spectral shift as well as quantum yield.[23] Indeed, in this case, the unique electric field and dipole characteristics of a peptide in the α-

dx.doi.org/10.1021/jp500883s | J. Phys. Chem. B 2014, 118, 2351−2359

helical structure[24] are likely to substantially influence the TPA properties of the labeled system (Figure 6).

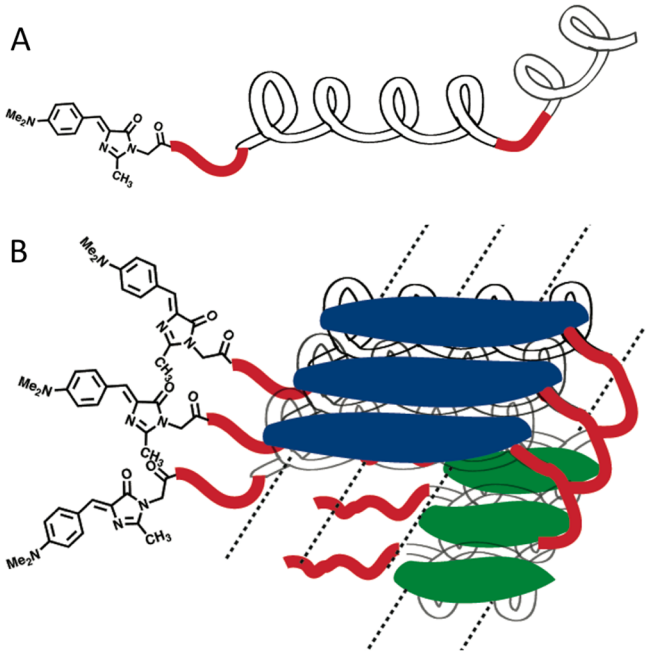

Figure 6. Representation of amyloid-β(1−42) labeled at the N-terminus with DMC. (a) At low concentration, significant quantities of α-helix are present. (b) At high concentration, significant β-strand/sheet structures result. Graphic shows only the basic interaction of several peptide units for clarity; dotted lines indicate further interactions likely occurring.

Isolated organic molecules have cross-section values that are independent of concentration if prepared in dilute solution. As shown in Figure 7, however, the values for DMC-Aβ(1−42) peptide system differed significantly depending on concentration. One can clearly see a factor of 6 drop in the two-photon cross section as a function of concentration in the range of 0.5−5 μM in Figure 7. This response demonstrates a good dynamic range for this methodology. These differences indicate that the critical determining factors in the TPA cross sections are the conformational changes in the secondary structure of the amyloid peptide and attached DMC as aggregation proceeds.

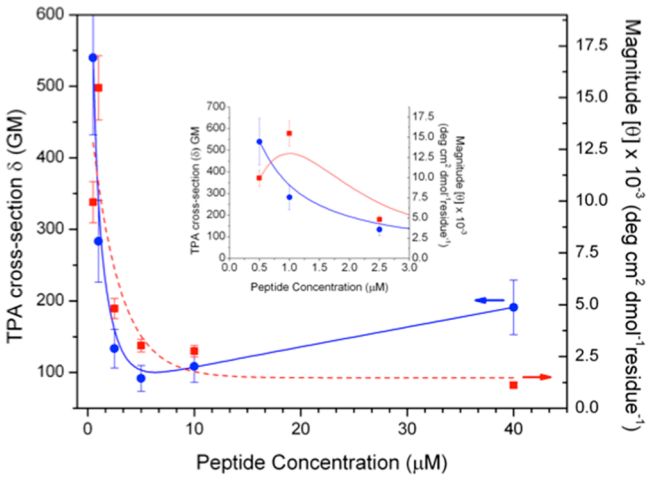

Figure 7. Two-photon absorption cross sections and molar ellipticity as functions of peptide concentration. Blue circles, two-photon absorption cross sections; red squares, molar ellipticity values as determined from CD data collected at 222 nm. Inset graph: Enlargement of low-concentration data. Lines are meant as guides and are not necessarily mathematical fits. Error bars represent standard errors associated with multiple TPA measurements and a 10% uncertainty for CD.

To explain the anomalous behavior of the TPA spectra, we applied a density functional theory quadratic response at the CAMB3LYP/6-31G(d,p)[25−27] level to determine the two-photon absorption (TPA) cross section of DMC clusters. This calculation ignores the peptide and assumes that DMC cluster formation is the origin of the concentration dependence of the results. Response calculations were performed using a local version of the DALTON package.[28] Because of the size of the DMC molecule, we considered clusters consisting of up to three DMC molecules in various configurations. DMC clusters were built using the gas-phase equilibrium structure of the DMC molecule optimized at the MP2/6-31G(d,p) level using the GAMESS package.[29] Reported distances were measured between the centers of mass of the monomers.

For the dimer calculations, we considered orientations of the DMC molecules based on the alignment of the transition dipole moment between the ground state and the first excited state. Because the transition dipole is aligned along the molecular plane (for the transitions of interest here), we considered three spatial orientations with DMC molecules in-plane parallel to each other, stacked, and placed in a line. The two first orientations lead to a parallel alignment, and the last leads to a linear alignment of the transition dipole moments. For the trimer, we considered only the planar orientation.

Figure 8 displays the TPA probability for the DMC dimers (top panel) and trimers (middle panel) for three monomer separations set to 7.5 Å (blue), 10 Å (orange), and 15 Å (green) in the planar parallel orientation. Both panels include the monomer TPA probability (red) for comparison. The bottom panel of Figure 8 displays the comparison of the TPA probabilities for monomer, dimer, and trimer for a 7.5-Å separation between monomers. The ordinate of each panel is scaled by the number of monomers and normalized to the TPA of the monomer. TPA probabilities for stacked and linear orientations of dimers are included in the Supporting Information (Figure S2). The TPA probability is presented with a Lorentzian line shape superimposed on the quadratic-response TPA data. We used a broadening factor (excited-state width) of γ = 0.05 eV for all data. The top panel, in addition to quadratic-response TPA values (solid lines), includes also TPA probabilities calculated using a three-state model that generalizes earlier models developed by Alam et al.[30]

The various orientations of the DMC clusters exhibit different behaviors of the two-photon absorption probability with respect to the intermolecular distance in the cluster. The planar (and stacked) orientation with parallel transition dipoles shows a decrease in the TPA probability for shorter separations. The opposite behavior is seen for the linear orientation, with transition dipoles aligned head to tail, for which the TPA of the dimer increases for shorter separations. The three-state model applied in this study is based on a sum-over-states model restricted to two excited states in which the TPA probability depends on the transition dipole moment and the excited-state moment and is a function of their mutual orientation.[30] Whereas the mutual orientation remains similar for all considered distances between monomers, it is the dipole

dx.doi.org/10.1021/jp500883s | J. Phys. Chem. B 2014, 118, 2351−2359

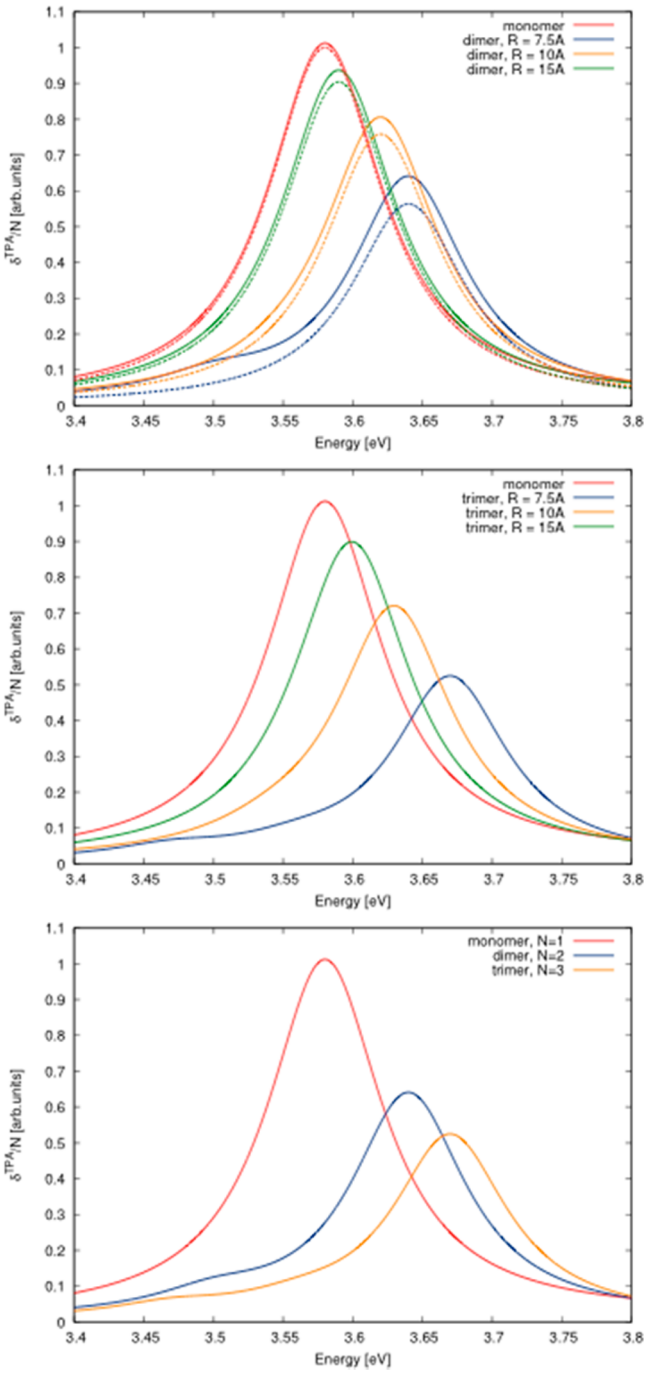

Figure 8. Two-photon absorption probability for DMC clusters in planar parallel orientation for separations between monomers set to 7.5 Å (blue), 10 Å (orange), and 15 Å (green) presented in comparison with the TPA of the monomer (red). All values are normalized to the TPA of the monomer. Top panel presents dimers; middle panel, trimers; and bottom panel, comparison of monomer, dimer, and trimer for 7.5-Å separation. Solid lines represent DFT quadratic response data, and dashed lines represent values obtained using a three-state model.

moments that play the crucial role in the TPA dependence. Two dipoles aligned parallel mutually induce additional moments that have a direction opposite to that of the initial dipoles. The total dipole moment, being a sum of the initial and induced dipoles, is therefore smaller than the sum of the two noninteracting dipoles, leading to a decrease in the TPA probability for short separations where the induction is the strongest. The opposite phenomenon occurs for linearly aligned dipoles, where the induced dipoles have the same direction as the initial dipoles, leading to a total dipole moment that is larger than that for two noninteracting systems. Linear orientations will therefore lead to an increase in TPA for short separations of monomers. The same argument holds for larger clusters, with the induction effect becoming increasingly important as the number of monomers in the cluster increases. Because the induction falls off as $1/R^3$, the change in the TPA due to the presence of other monomers eventually saturates as the number of monomers in the cluster increases. Unfortunately, it is not possible to study clusters of TPA larger than trimers; however, calculations we have done for smaller molecules (not presented) suggest that reductions in TPA cross section comparable to what were observed are possible for large clusters.

Enhanced TPA cross sections for head-to-tail dimer structures and chains have been noted in earlier calculations.[31,32] Also, it has been experimentally demonstrated[33] that there is a potential for through-space chromophore interactions to enhance two-photon absorption cross sections for polar arylamine structures designed to dimerize in solution. The interaction distances for these systems are on the order of interstrand distances typically found in amyloid structures, providing the potential for head-to-tail chromophore−chromophore or chromophore−amino acid interactions. Detailed investigations examining such interactions were undertaken using time-resolved fluorescence and anisotropy measurements to understand how concentration changes affect the adopted aggregate conformations and chromophore interactions. In contrast to this earlier work, the present work on parallel or stacked arrangements of chromophores that leads to reduced TPA has apparently not been considered.

Comparison of Two-Photon Spectroscopy to Circular Dichroism. A relative comparison between CD and TPA shows that the two-photon absorption cross sections measured as a function of peptide concentration show very similar trends to the relative change in ellipticity of the peptides found using CD over a wide concentration distribution (Figure 7). However, when the comparison is focused on the lowest concentrations, the trend does not demonstrate the same behavior, as an even higher-intensity signal is observed using two-photon absorption at 0.5 μM. This contrasts with the plateauing seen in the CD data and is an indication that the methodology has better sensitivity to small changes in conformation or aggregation at very dilute solution concentrations as well with small relative differences in concentration. As demonstrated, the inherent limitations to the collection of data for quantitative secondary structure determination using peptide concentrations at submicromolar values present large challenges for the observation of solutions with biologically relevant concentrations. A two-photon excited methodology clearly can resolve these levels while avoiding some of the other challenges presented in collecting CD data, such as background sources of absorption from other solution additives and buffers.[34] The implication of this finding for our methodology could be significant, as it indicates that a two-photon-based technique might be able to reveal answers to the very specific conformational questions about amyloid-β(1−42) at dilute, biologically relevant concentrations inaccessible with other techniques.

dx.doi.org/10.1021/jp500883s | J. Phys. Chem. B 2014, 118, 2351−2359

Fluorescence Lifetimes and Anisotropy. Two-photon spectroscopy can be a sensitive probe of changes in secondary structure in peptide aggregates and over a broad size- and distance-dependent range. It has been shown that fluorescence upconversion measurements can provide compelling evidence of strong intramolecular interactions and coherent energy-transfer dynamics in aggregate macromolecular structures,[35] making it a very useful technique for investigating the interactions of DMC in the amyloid peptide system.

Shown in Figure 9 are the fluorescence decay profiles for free DMC and three different peptide concentrations. The decay

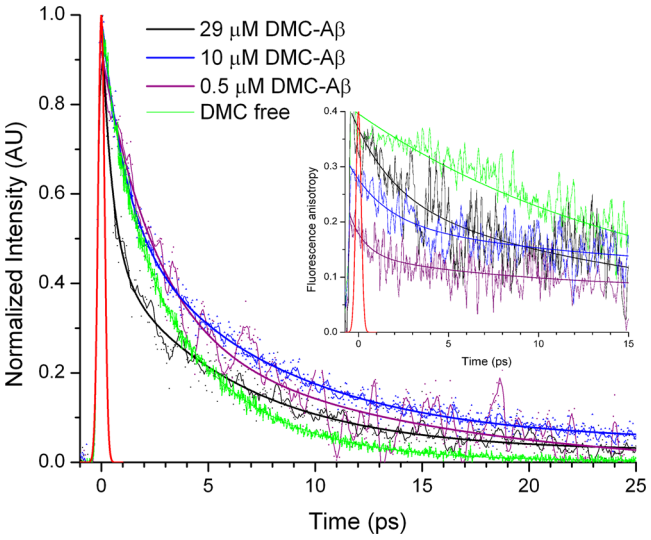

Figure 9. Fluorescence decays of various concentrated DMC-Aβ solutions as compared with that of "free" DMC. Inset: Fluorescence anisotropic decays of various DMC-Aβ solutions as compared with that of free DMC. Black, 29 μM DMC-Aβ; blue, 10 μM DMC-Aβ; purple, 0.5 μM DMC-Aβ; green, free DMC; red, instrument response function.

profile for the free dye in PBS shows the expected single-exponential decay of fluorescence on a time scale of ~10 ps (Table 3). For the 0.5 and 10 μM peptide concentrations, the decays are similar to that of free DMC, showing a biexponential profile that relaxes to the ground state at ~10 ps. This suggests that any local effects surrounding the functionalized peptide do not inhibit the decay profiles for these two concentrations. In the case of the two-photon absorption effects (see above), there was a dramatic difference in the cross sections for these two concentrations, suggesting that, at the lower concentrations, the two-photon absorption method is sensitive changes in the transition from α-helix to β-sheet formation where time-resolved fluorescence shows less sensitivity in this concentration regime. Interestingly, an extended fast decay component was observed for the highest concentration (29 μM) that was not as strongly pronounced at lower concentrations. This also parallels the two-photon measurements where, at very high concentrations, the change in the cross section was less substantial. The extended fast component might be due to a change in the local environment surrounding the dye attached to the peptide such as a further change (or transition) in the conformation. Previous reports with ultrafast fluorescence upconversion on organic dipolar chromophores attached to other macromolecular architectures have observed that an increase in the fast component of the decay might suggest a change in the region surrounding the chromophore.[16] Indeed, this might be possible here because peptide conformational changes occur that affect chromophore−chromophore interactions.

For the 0.5 and 10 μM peptide concentrations, the decays were similar to that of free DMC, showing a biexponential profile that relaxed to the ground state at ~10 ps. This suggests that any local effects surrounding the functionalized peptide do not inhibit the decay profiles for these two concentrations. In the case of the two-photon absorption effects (see above), there was a dramatic difference in the cross sections for these two concentrations. Thus, at the lower concentrations, the two-photon absorption method is sensitive to changes in the transition from α-helix to β-sheet formation, whereas time-resolved fluorescence shows less sensitivity in this concentration regime. Interestingly, an extended fast decay component was observed for the highest concentration (29 μM) that was not as strongly pronounced at lower concentrations. This also contrasts with the two-photon measurements, where, at very high concentrations, the change in the cross section was less substantial. The extended fast component might be attributed to a change in the local environment surrounding the dye attached to the peptide such as a further change (or transition) in conformation. Previous reports with ultrafast fluorescence upconversion on organic dipolar chromophores attached to other macromolecular architectures have observed that an increase in the fast component of the decay correlates with a change in the region surrounding the chromophore.[16] Indeed, this might be possible here because peptide conformational changes occur that affect chromophore−chromophore interactions.

To further understand the energy-transfer mechanism in these aggregated peptide systems, ultrafast fluorescence anisotropy decay measurements were also carried out. The anisotropy decay dynamics for the same set of aggregating samples are shown in the Figure 9 inset. The free chromophore decay is expected to give the slowest relaxation on this time scale (Table 3). The 29 μM system has an extensive fast component that persists up to 3 ps. The fast component in the two more dilute peptide samples vanishes on a shorter time

Table 3. Fluorescence Lifetimes for DMC-Labeled Amyloid-β(1−42) Compared to Those of Free DMC[a,b]

	lifetime (ps)		anisotropy (ps)		
peptide concentration (μM)	τ_1	τ_2	τ_1	τ_2	r_0[c]
29	0.83 ± 0.05	7.1 ± 0.2	2.2 ± 0.9	17 ± 7	0.36
10	1.10 ± 0.07	7.2 ± 0.3	1.9 ± 0.5	16 ± 5	0.25
0.5	2.2 ± 0.8	10 ± 3	0.9 ± 0.5	10 ± 4	0.15
0[d]	1.07 ± 0.07	4.19 ± 0.04	–	16 ± 1	0.36

[a]Peptide solutions prepared to have a HFIP/PBS ratio of 80:20. [b]Error associated with the uncertainty in the exponential fitting of each decay. [c]Measured initial anisotropy of the solution. [d]Free DMC.

dx.doi.org/10.1021/jp500883s | J. Phys. Chem. B 2014, 118, 2351−2359

scale near 1 ps. The existence of this fast component in the anisotropy decay is not related to rotational diffusion, suggesting intermolecular energy transfer between dye molecules in the aggregate. As noted in the calculations and experimental results above, we already observed an increase in the two-photon cross section for the high-concentration aggregated system as compared to the free dye in dilute solution. Indeed, with fluorescence anisotropy decay measurements, the time scale of the fluorescence depolarization process in the peptide−chromophore system might be a signature of excitonic states with large transition dipoles[36] in the parallel orientation favorable for increased TPA compared to the isolated chromophore. This kind of interaction, due to the nature of its relaxation rate, is not commonly observed in steady-state experiments. Indeed, although this fast component, which is indicative of a fast energy transfer, is faster than one would suggest for rotational motion,[37] it might be understood in the context of the Förster model.[38]

The initial anisotropy values for the various solutions showed a significant effect of concentration, with a large depression noted in the case of the least concentrated 0.5 μM sample (Table 3). This would indicate a fast depolarizing process that occurs very quickly within the time of the instrument response function. For the 0.5−5 μM solutions, the results strongly suggest that a significant chromophore−chromophore interaction is occurring, consistent with the computational modeling on the interactions of DMC chromophores. The suggestion from the CD data that significant α-helical structure can be found in monomeric species provides some support that the peptides might be conformationally ordered in such a way that the inteactiron strength is high. However, the highest concentration 29 μM solution lacks the same significant depolarization seen at the lowest concentration. With significantly lower two-photon absorption cross sections (at 40 μM) and far slower fluorescence depolarization, this would indicate that chromophore interactions are slightly diminished in this state. The additional order and stability provided by increased β-sheet secondary structure does not bring the more disordered N-terminus region of the peptide into a position favorable for strong interactions with other chromophores, as evidenced by these results. The intermediate concentrations studied gave rise, as expected, to data between the two concentration extremes with anisotropic decay (for the 10 μM sample) similar to that observed for 29 μM and for a range of samples studied using TPA, with cross sections diminished with increasing β-sheet content, as indicated by CD. These results are consistent with the hypothesized complex secondary structure that could lead to a number of different of conformers. The extent of depolarization and fluorescence decay is consistent with an intermediate oligomer structure between ordered extremes. Overall, the combined results of time-resolved fluorescence and two-photon absorption spectroscopy demonstrate a high level of sensitivity for changes in amyloid-β conformation as it aggregates from monomers to soluble oligomers.

CONCLUSIONS

The results presented in this report examine the earliest conformational dynamics of amyloid-β peptide utilizing a combined approach of two-photon absorption and time-resolved fluorescence spectroscopy. A large two-photon cross section was observed for the attached dye−peptide system [DMC-labeled Aβ(1−42) segment] at very low concentrations. The advantages of shifting the excitation source out of the high-energy ultraviolet region where sources of background absorption are much more prevalent coupled with the inherent sensitivity of TPA makes it a powerful alternative technique to CD for the characterization of the early conformational changes of aggregating peptides. A relative comparison of our TPA studies with circular dichroism spectroscopy showed that the two-photon methodology has greater sensitivity than CD to conformational changes taking place at concentrations of ∼1 μM and lower. The two-photon cross section decreases with increasing concentration of the dye−peptide system in the range from 0.5 to 5 μM. Accurate electronic structure calculations together with a three-state model demonstrated that the TPA cross section decreases with increasing aggregation when the chromophores are stacked or parallel, indicating the influence of aggregation on the results. Fluorescence lifetime and depolarization studies indicate that Förster-type energy transfer can be observed, with results correlating well with the chromophore interactions evidenced by the TPA cross sections. Additional development of the methodology could result in broadened applications beyond solution-phase studies by utilizing two-photon near-field scanning optical microscopy to characterize larger insoluble aggregates, thereby yielding a technique that has the ability to monitor aggregation over the full fibrillization pathway (Figure 1) and the potential to answer some of the prevailing questions that remain about the conformational dynamics of many of the peptides that result in neurodegenerative disease.

ASSOCIATED CONTENT

Supporting Information

Additional peptide characterization and figures associated with two-photon modeling. This material is available free of charge via the Internet at http://pubs.acs.org.

AUTHOR INFORMATION

Corresponding Author

*Tel.: 734-647-0274. Fax: 734-615-3790. E-mail tgoodson@umich.edu.

Notes

The authors declare no competing financial interest.

ACKNOWLEDGMENTS

We thank the National Science Foundation (T.G.III, Grant DMR 1306815), the Army Research Office (T.G.III, Grant W911NF-13-1-0314), and the AFOSR (G.S., Grant FA9550-14-1-0053) for support of this work.

REFERENCES

(1) Ono, K.; Condron, M. M.; Teplow, D. B. Structure−Neurotoxicity Relationships of Amyloid β-Protein Oligomers. *Proc. Natl. Acad. Sci. U.S.A.* **2009**, *106*, 14745−14750.

(2) Dobson, C. Protein Folding and Misfolding. *Nature* **2003**, *426*, 884−890.

(3) Nag, S.; Sarkar, B.; Bandyopadhyay, A.; Sahoo, B.; Sreenivasan, V. K. A.; Kombrabail, M.; Muralidharan, C.; Maiti, S. The Nature of the Amyloid-Beta Monomer and the Monomer−Oligomer Equilibrium. *J. Biol. Chem.* **2011**, *286*, 13827−13833.

(4) Barrow, C.; Yasuda, A.; Kenny, P.; Zagorski, M.; Wright, P. Solution Conformations and Aggregational Properties of Synthetic Amyloid β-Peptides of Alzheimer's Disease: Analysis of Circular Dichroism Spectra. *J. Mol. Biol.* **1992**, *225*, 1075−1093.

(5) Levine, H. Thioflavine T Interaction With Synthetic Alzheimer's Disease β-Amyloid Peptides: Detection of Amyloid Aggregation in Solution. *Protein Sci.* **1993**, *2*, 404−410.
(6) Bartolini, M.; Naldi, M.; Fiori, J.; Valle, F.; Biscarini, F.; Nicolau, D. V.; Andrisano, V. Kinetic Characterization of Amyloid-Beta 1−42 Aggregation with a Multimethodological Approach. *Anal. Biochem.* **2011**, *414*, 215−225.
(7) Vestergaard, M. d.; Hamada, T.; Saito, M.; Yajima, Y.; Kudou, M.; Tamiya, E.; Takagi, M. Detection of Alzheimer's Amyloid Beta Aggregation by Capturing Molecular Trails of Individual Assemblies. *Biochem. Biophys. Res. Commun.* **2008**, *377*, 725−728.
(8) Kirkitadze, M.; Condron, M.; Teplow, D. Identification and Characterization of Key Kinetic Intermediates in Amyloid β-Protein Fibrillogenesis. *J. Mol. Biol.* **2001**, *312*, 1103−1119.
(9) Walsh, D. M.; Hartley, D. M.; Kusumoto, Y.; Fezoui, Y.; Condron, M. M.; Lomakin, A.; Benedek, G. B.; Selkoe, D. J.; Teplow, D. B. Amyloid β-Protein Fibrillogenesis. *J. Biol. Chem.* **1999**, *274*, 25945−25952.
(10) Allsop, D.; Swanson, L.; Moore, S.; Davies, Y.; York, A.; El-Agnaf, O. M. A.; Soutar, I. Fluorescence Anisotropy: A Method for Early Detection of Alzheimer β-Peptide (Aβ) Aggregation. *Biochem. Biophys. Res. Commun.* **2001**, *285*, 58−63.
(11) Rolinski, O. J.; Amaro, M.; Birch, D. J. S. Early Detection of Amyloid Aggregation Using Intrinsic Fluorescence. *Biosens. Bioelectron.* **2010**, *25*, 2249−2252.
(12) Varnavski, O.; Yan, X.; Mongin, O.; Blanchard-Desce, M.; Goodson, T. Strongly Interacting Organic Conjugated Dendrimers with Enhanced Two-Photon Absorption. *J. Phys. Chem. C* **2007**, *111*, 149−162.
(13) Drobizhev, M.; Karotki, A.; Dzenis, Y.; Rebané, A.; Suo, Z.; Spangler, C. W. Strong Cooperative Enhancement of Two-Photon Absorption in Dendrimers. *J. Phys. Chem. B* **2003**, *107*, 7540−7543.
(14) Brown, O.; Lopez, S.; Fuller, A.; Goodson, T., III. Formation and Reversible Dissociation of Coiled Coil of Peptide to the C-Terminus of the HSV B5 Protein: A Time-Resolved Spectroscopic Analysis. *Biophys. J.* **2007**, *93*, 1068−1078.
(15) Wang, Y.; Goodson, T., III. Early Aggregation in Prion Peptide Nanostructures Investigated by Nonlinear and Ultrafast Time-Resolved Fluorescence Spectroscopy. *J. Phys. Chem. B* **2007**, *111*, 327−330.
(16) Wang, Y.; Clark, T. B.; Goodson, T., III. Two-Photon and Time-Resolved Fluorescence Conformational Studies of Aggregation in Amyloid Peptides. *J. Phys. Chem. B* **2010**, *114*, 7112−7121.
(17) Clark, T. B.; Orr, M. E.; Flynn, D. C.; Goodson, T., III. Synthesis and Optical Properties of Two-Photon Absorbing GFP-Type Probes. *J. Phys. Chem. C* **2011**, *115*, 7331−7338.
(18) Theodorou, V.; Skobridis, K.; Tzakos, A. G.; Ragoussis, V. A Simple Method for the Alkaline Hydrolysis of Esters. *Tetrahedron Lett.* **2007**, *48*, 8230−8233.
(19) Xu, C.; Williams, R.; Zipfel, W.; Webb, W. Multiphoton Excitation Cross-Sections of Molecular Fluorophores. *Bioimaging* **1996**, *4*, 198−207.
(20) Varnavski, O.; Goodson, T. Femtosecond Fluorescence Dynamics and Molecular Interactions in a Water-Soluble Nonlinear Optical Polymeric Dye. *Chem. Phys. Lett.* **2000**, *320*, 688−696.
(21) Tolbert, L. M.; Baldridge, A.; Kowalik, J.; Solntsev, K. M. Collapse and Recovery of Green Fluorescent Protein Chromophore Emission through Topological Effects. *Acc. Chem. Res.* **2012**, *45*, 171−181.
(22) Bateman, D. A.; McLaurin, J.; Chakrabartty, A. Requirement of Aggregation Propensity of Alzheimer Amyloid Peptides for Neuronal Cell Surface Binding. *BMC Neurosci.* **2007**, *8*, 29−41.
(23) Albota, M.; Beljonne, D.; Brédas, J.-L.; Ehrlich, J. E.; Fu, J.-Y.; Heikal, A. A.; Hess, S. E.; Kogej, T.; Levin, M. D.; Marder, S. R.; McCord-Maughon, D.; Perry, J. W.; Röckel, H.; Rumi, M.; Subramaniam, G.; Webb, W. W.; Wu, X.-L.; Xu, C. Design of Organic Molecules with Large Two-Photon Absorption Cross Sections. *Science* **1998**, *281*, 1653−1656.
(24) Hol, W. G. J.; van Duijnen, P. T.; Berendsen, H. J. C. The α-Helix Dipole and the Properties of Proteins. *Nature* **1978**, *273*, 443−446.
(25) Yanai, T.; Tew, D. P.; Handy, N. C. A New Hybrid Exchange-Correlation Functional Using the Coulomb-Attenuating Method (CAM-B3LYP). *Chem. Phys. Lett.* **2004**, *393*, 51−57.
(26) Hehre, W. J.; Ditchfie, R.; Pople, J. A. Self-Consistent Molecular Orbital Methods. XII. Further Extensions of Gaussian-Type Basis Sets for Use in Molecular Orbital Studies of Organic Molecules. *J. Chem. Phys.* **1972**, *56*, 2257−2261.
(27) Harihara, P. C.; Pople, J. A. Influence of Polarization Functions on Molecular-Orbital Hydrogenation Energies. *Theor. Chim. Acta* **1973**, *28*, 213−222.
(28) *DALTON. A Molecular Electronic Structure Program*, release 2.0; National Supercomputer Centre: Linköping, Sweden, 2005; see http://www.kjemi.uio.no/software/dalton/dalton.html.
(29) Schmidt, M. W.; Baldridge, K. K.; Boatz, J. A.; Elbert, S. T.; Gordon, M. S.; Jensen, J. H.; Koseki, S.; Matsunaga, N.; Nguyen, K. A.; Su, S. J.; Windus, T. L.; Dupuis, M.; Montgomery, J. A. General Atomic and Molecular Electronic-Structure System. *J. Comput. Chem.* **1993**, *14*, 1347−1363.
(30) Alam, M. M.; Chattopadhyaya, M.; Chakrabarti, S. Solvent Induced Channel Interference in the Two-Photon Absorption Process—A Theoretical Study with a Generalized Few-State-Model in Three Dimensions. *Phys. Chem. Chem. Phys.* **2012**, *14*, 1156−1165.
(31) Ohira, S.; Brédas, J. L. Porphyrin Dimers: A Theoretical Understanding of the Impact of Electronic Coupling Strength on the Two-Photon Absorption Properties. *J. Mater. Chem.* **2009**, *19*, 7545−7550.
(32) Trohalaki, S.; Kedziora, G. S.; Pachter, R. Molecular Dynamics Simulation of Two Photon-Absorbing Polyimides: Evidence for the Formation of Intra- and Inter-Chain Dimers. *Polymer* **2012**, *53*, 3421−3425.
(33) Terenziani, F.; Parthasarathy, V.; Pla-Quintana, A.; Maishal, T.; Caminade, A.-M.; Majoral, J.-P.; Blanchard-Desce, M. Cooperative Two-Photon Absorption Enhancement by Through-Space Interactions in Multichromophoric Compounds. *Angew. Chem., Int. Ed.* **2009**, *121*, 8847−8850.
(34) Greenfield, N. J. Using Circular Dichroism Spectra to Estimate Protein Secondary Structure. *Nat. Protocols* **2007**, *1*, 2876−2890.
(35) Varnavski, O. P.; Ostrowski, J. C.; Sukhomlinova, L.; Twieg, R. J.; Bazan, G. C.; Goodson, T. Coherent Effects in Energy Transport in Model Dendritic Structures Investigated by Ultrafast Fluorescence Anisotropy Spectroscopy. *J. Am. Chem. Soc.* **2002**, *124*, 1736−1743.
(36) Klugkist, J. A.; Malyshev, V. A.; Knoester, J. Scaling and Universality in the Optics of Disordered Exciton Chains. *Phys. Rev. Lett.* **2008**, *100*, 216403.
(37) Bora, R. P.; Prabhakar, R. Translational, Rotational and Internal Dynamics of Amyloid β-Peptides (Aβ40 and Aβ42) from Molecular Dynamics Simulations. *J. Chem. Phys.* **2009**, *131*, 155103−155111.
(38) Scholes, G. D. Long-Range Resonance Energy Transfer in Molecular Systems. *Annu. Rev. Phys. Chem.* **2003**, *54*, 57−87.